

Figure 4. Quantification of PCR products. Results were obtained by employing the same conditions as shown in Figure 3 using 5'-³²P-labeled primer probes. Aliquots were removed after every cycle and subsequently analyzed by denaturing PAGE using phosphorimaging technology. The percentage of product relative to the overall radioactivity in one lane was plotted against the number of cycles. Error bars derive from repeated experiments. A) Results obtained with probes bearing unmodified thymidine residues at the 3'-primer end. B) Results obtained with primer probes bearing 4'-vinylated thymidine residues at the 3'-primer end. The respective primer/template duplexes were indicated by the following symbols: ● TR/A, ▼ TR/G, ▲ TR/C, ■ TR/T.^[7]

es that are not easily accessible with unmodified substrates. Considering recent developments in the use of real-time quantitative PCR as an analytical tool for detecting variations in nucleotides,^[11] these findings should have significant impact on the development of reliable and robust methods.

Received: July 15, 2002 [Z19731]

- [1] For example: a) A. D. Ross, *Nature* **2000**, *405*, 857–865; b) J. J. McCarthy, R. Hilfiker, *Nat. Biotechnol.* **2000**, *18*, 505–508; c) W. E. Evans, M. V. Relling, *Science* **1999**, *286*, 487–491; d) P. W. Kley, E. S. Vesell, *Science* **1998**, *281*, 1820–1821.
- [2] For example: a) M. M. Shi, *Clin. Chem.* **2001**, *47*, 164–172; b) I. G. Gut, *Hum. Mutat.* **2001**, *17*, 475–492; c) M. Chicurel, *Nature* **2001**, *412*, 580–582; d) P. Y. Kwok, *Annu. Rev. Genomics Hum. Genet.* **2001**, *2*, 235–258.
- [3] D. Y. Wu, L. Ugozzoli, B. K. Pal, R. B. Wallace, *Proc. Natl. Acad. Sci. USA* **1989**, *86*, 2757–2760.
- [4] For example: a) Z. Guo, Q. Liu, L. M. Smith, *Nat. Biotechnol.* **1997**, *15*, 331–335; b) Y. Ishikawa, K. Tokunaga, K. Kashiwase, T. Akaza, K. Tadokoro, T. Juji, *Hum. Immunol.* **1995**, *42*, 315–318; c) P. R. Wenham, C. R. Newton, W. H. Price, *Clin. Chem.* **1991**, *37*, 241–244; d) C. R. Newton, A. Graham, L. E. Heptinstall, S. J. Powell, C. Summers, N. Kalsheker, J. C. Smith, A. F. Markham, *Nucleic Acids Res.* **1989**, *17*, 2503–2516.
- [5] a) D. Summerer, A. Marx, *Angew. Chem.* **2001**, *113*, 3806–3808; *Angew. Chem. Int. Ed.* **2001**, *40*, 3693–3695; b) D. Summerer, A. Marx, *J. Am. Chem. Soc.* **2002**, *124*, 910–911; c) M. Strerath, D. Summerer, A. Marx, *ChemBioChem* **2002**, *3*, 578–580.
- [6] E. T. Kool, *Annu. Rev. Biochem.* **2002**, *71*, 191–219.
- [7] Detailed experimental procedures as well as DNA sequences applied are provided in the Supporting Information.
- [8] All DNA polymerases experiments conducted were done in the sequence context of human acid ceramidase comprising the recently discovered mutation at A107. See: J. Bär, T. Linke, K. Ferlinz, U. Neumann, E. H. Schuchman, K. Sandhoff, *Hum. Mutat.* **2001**, *17*, 199–209.
- [9] N. Nomura, S. Shuto, M. Tanaka, T. Sasaki, S. Mori, S. Shigata, A. Matsuda, *J. Med. Chem.* **1999**, *42*, 2901–2908.
- [10] R. T. Pon in *Current Protocols in Nucleic Acids Chemistry* (Eds.: S. L. Beaucage, D. E. Bergstrom, G. D. Glick, R. A. Jones), Wiley, **2000**, chapters 3.2.1–3.2.23.
- [11] *Rapid Cycle Real-Time PCR* (Eds.: S. Meuer, C. Wittwer, K. Nakagawara), Springer, Berlin, **2001**.

Detection of Individual p53-Autoantibodies by Using Quenched Peptide-Based Molecular Probes**

Hannes Neuweiler, Andreas Schulz, Andrea C. Vaiana, Jeremy C. Smith, Sepp Kaul, Jürgen Wolfrum, and Markus Sauer*

The development of new fast and sensitive assay formats for cancer diagnosis is one of the most challenging tasks in biomedical analysis. Since p53-autoantibodies are independent and highly specific tumor markers with a substantial potential for early-stage diagnosis they have become a focus of modern cancer diagnosis.^[1] Here we report on the development of a sensitive and fast assay for p53-autoantibodies using a novel single-molecule fluorescence spectroscopic method. The method involves detection of reversible fluorescence quenching of dyes by tryptophan residues in labeled short peptides derived from the antibody recognition sequence of the p53 protein. The effectiveness of these peptide-based molecular probes for early-stage diagnosis and follow-up of malignant diseases is demonstrated by the detection of individual p53-autoantibodies directly in sera of cancer patients in the concentration range relevant for clinical tests. Gene mutation in p53—the guardian of the genome^[2]—is the most frequently found abnormality in human cancer^[3] and often triggers the immune system to produce antibodies directed against the nuclear tumor suppressor protein p53—the DNA transcript of the p53 gene. The presence of p53-autoantibodies in human serum validates a malignant disease with a specificity of 100% if autoimmune diseases are neglected.^[1] Commonly, the enzyme-linked immunosorbent assay (ELISA) technique is used as heterogeneous assay format to detect p53-autoantibodies, whose detection limit lies in the range of 10^{−9}–10^{−11} M. The major disadvantages of this method are that it is slow (several hours) and, due to the requirement of recombinant p53, expensive.

Lubin and co-workers have shown that the immune response of cancer patients is not directed against the mutated central segment of the p53 sequence, but rather is directed against a small subset of linear peptide epitopes localized mainly in the N-terminal region (the transactivation domain)

[*] Priv.-Doz. Dr. M. Sauer, H. Neuweiler, Dr. A. Schulz, Prof. Dr. J. Wolfrum
Physikalisch-Chemisches Institut
Universität Heidelberg
Im Neuenheimer Feld 253, 69120 Heidelberg (Germany)
Fax: (+49) 6221-54-4225
E-mail: sauer@urz.uni-heidelberg.de
A. C. Vaiana, Prof. Dr. J. C. Smith
IWR
Universität Heidelberg
Im Neuenheimer Feld 368, 69120 Heidelberg (Germany)
Dr. S. Kaul
Universitätsfrauenklinik Heidelberg
Voßstrasse 7, 69115 Heidelberg (Germany)

[**] The authors thank K.H. Drexhage for the oxazine derivative MR121, and the Volkswagen-Stiftung, the Forschungsschwerpunktprogramm of the Land Baden-Württemberg, and the Bundesministerium für Bildung, Wissenschaft, Forschung und Technologie for financial support.

of the protein chain.^[4] Hence, these peptides may be promising systems on which to base the development of a homogeneous fluorescence immunoassay.

The sequences of both peptide epitopes each contain a tryptophan residue. The indole derivative tryptophan is an efficient fluorescence quencher of several environment-sensitive fluorescent dyes, which absorb and emit in the red spectral region. Here we demonstrate that hydrophobic interactions of inherent tryptophan residues in peptide epitopes with fluorescent dyes and protein binding sites enable the design of efficiently quenched peptide-based molecular probes which indicate specific binding to antibodies by a strong increase in fluorescence.

We labeled both immunodominant epitopes of human p53 with a red-absorbing oxazine derivative MR121 (Figure 1 a) at the N-terminal ends of the peptides. Hydrophobic interactions lead to a peptide conformation in which the fluorescence of the oxazine dye is efficiently quenched by the nearby tryptophan residue; the relative fluorescence quantum yields $\Phi_{f,rel}$ are 0.38 (epitope I) and 0.21 (epitope II, Table 1). Shifts in absorption and emission spectra indicate ground- and excited-state interactions between tryptophan and the dye. In combination with time-resolved fluorescence measurements, which show nearly unchanged average decay times (Table 1), these data strongly support the expected static interaction of the dye with tryptophan residues, that is, the formation of non- or only weakly fluorescent charge-transfer complexes. The remaining fluorescence intensity can be explained by a dynamic equilibrium between a folded (quenched) and an open (unquenched) state of the conjugate. Measurements of the tryptophan fluorescence in the labeled peptides provide evidence for the suggested mechanism. The tryptophan residues in both peptides show a strongly reduced fluorescence quantum yield and a considerable blue shift in emission maximum (from 349 to 337 nm) upon dye conjugation (Figure 1 c).

The *in vitro* binding of the fluorescently labeled epitopes to antibodies was studied by using monoclonal mouse antibodies directed against the N-terminus of human p53. The mouse clones BP53-12,^[5] and Pab 1801^[6] recognize specifically the residues 20 to 25 of epitope I, and residues 46 to 55 of epitope II, respectively, in the human p53 sequence. As exemplified in Figure 1 d, the addition of an excess of antibody to the labeled epitopes leads to a strong increase in fluorescence intensity (Table 1). The specific recognition process of the antibody induces a conformational change in the peptide-probe and diminishes the tryptophan-dye contact. The suggested mechanism is depicted in Figure 2.

Upon addition of the antibody the emission maximum of the dye slightly shifts into the blue, which indicates, in contrast to the tryptophan fluorescence, a more hydrophilic environment of the dye (Table 1). To test the applicability of these peptide-based molecular probes for the quantification

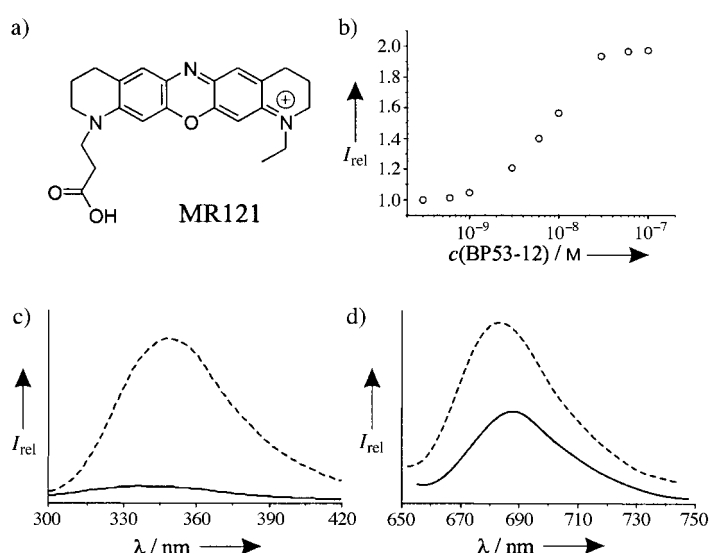


Figure 1. a) Molecular structure of the oxazine dye MR121 labeled to the N-terminal end of both epitopes (epitope I: amino acid residues 15 to 29, MR121-SQETFSDLWKLLPEN; epitope II: amino acid residues 46 to 65, MR121-SPDDIEQWFTEDPGPDEAPR). b) Relative fluorescence intensity (I_{rel}) of a 10^{-8} M solution of labeled epitope I in the presence of varying concentrations of the model antibody BP53-12. Measurements were performed in assay buffer. c) I_{rel} of tryptophan in labeled (—) and unlabeled (---) epitope I ($\lambda_{exc} = 290$ nm). d) I_{rel} of the dye in the labeled epitope I in the absence (—) and presence (---) of an excess of model antibody BP53-12 ($\lambda_{exc} = 640$ nm). Abbreviations for the amino acid residues are: A: alanine; D: aspartic acid; E: glutamic acid; F: phenylalanine; G: glycine; I: isoleucine; K: lysine; L: leucine; N: asparagine; P: proline; Q: glutamine; R: arginine; S: serine; T: threonine; W: tryptophan.

Table 1. Spectroscopic characteristics of the oxazine derivative MR121 and labeled peptide epitopes.^[a]

	λ_{abs} [nm]	λ_{em} [nm]	$\Phi_{f,rel}$	τ_1 [ns]	a_1	τ_2 [ns]	a_2	χ^2
MR121	661	673	1.00	1.85	1.00	—	—	1.066
MR121-epitope I	666	683	0.38	0.56	0.06	2.11	0.94	1.107
MR121-epitope I + BP53-12	666	680	0.76	1.06	0.06	2.16	0.94	1.105
MR121-epitope II	667	683	0.21	0.51	0.09	2.00	0.91	1.138
MR121-epitope II + PAb 1801	666	679	0.56	0.61	0.09	1.89	0.91	1.085

[a] Measurements were performed in assay buffer (100 mM sodium phosphate, pH 7.7, 0.3 mg mL⁻¹ albumin, 0.05 % Tween 20) at room temperature. λ_{abs} and λ_{em} are the absorption and the emission maxima of the measured probes, $\Phi_{f,rel}$ denotes the relative fluorescence quantum yield, and τ_i the fluorescence lifetimes with corresponding amplitudes a_i .

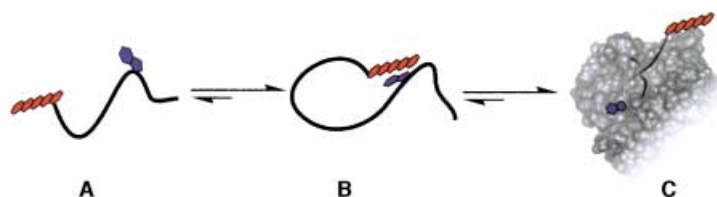


Figure 2. Principle of operation of the peptide-based molecular probes. Driven by the hydrophobic effect the peptide adopts a conformation (B) in which the dye interacts with the tryptophan residue. The quenched conformation coexists in an equilibrium with an open, less quenched conformation (A). Upon specific binding to the antibody binding site, the peptide adopts a new conformation (C), and charge-transfer interactions between tryptophan and the dye are diminished. As a consequence, the fluorescence intensity increases.

of antibodies in homogeneous solution we monitored the fluorescence intensity of 10^{-8} M solutions of the two labeled epitopes in the presence of different antibody concentrations. As depicted for epitope I in Figure 1 b, antibodies can be

easily detected by the increased fluorescence intensity, down to concentrations as low as a few nanomolar. These data suggest that the epitopes rearrange their conformation upon binding to the model antibody: the tryptophan residue shows strong interactions with the antibody binding pocket accompanied by reduced fluorescence quenching (Figure 2).

To increase detection sensitivity, we implemented confocal fluorescence microscopy. The application of a small excitation/detection volume reduces considerably elastic and inelastic scattering as well as background fluorescence. The use of a detection volume of about 1 fL enables the observation of single molecules in 10^{-9} to 10^{-12} M solutions. Hence, single molecules diffusing through the detection volume can be observed as fluorescence bursts with high signal-to-background ratios.^[7] In combination with red, pulsed diode lasers as excitation sources and fluorescent dyes emitting in the far red spectral region, this technique represents a valuable method for measurements in human serum samples.^[8] Furthermore, since single-molecule spectroscopy allows one to detect subpopulations even with only slightly changed spectroscopic characteristics it represents the technique of choice for discriminating between bound and free labeled epitopes through their different fluorescence intensities, that is, burst sizes.^[9] Details of the experimental set-up and data analysis are described in reference [10]. Figure 3 shows fluorescence intensity time traces of 5×10^{-11} M solutions of the two labeled epitopes in absence and presence of different concentrations of model antibodies. The quenched epitopes exhibit only

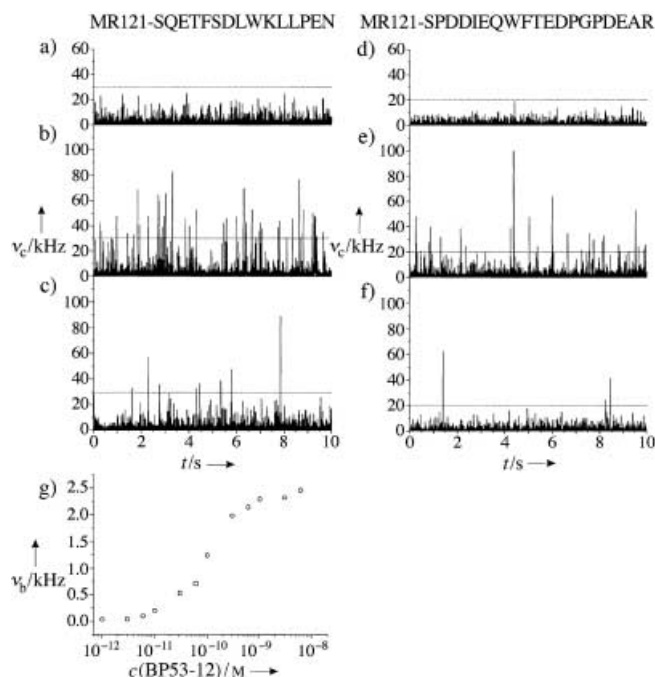


Figure 3. Fluorescence signals (count rate ν_c versus time t) observed from 5×10^{-11} M solutions of epitope I (left side) and epitope II (right side) in assay buffer in the absence (a, d) and presence of 10^{-9} M (b, e) and 10^{-10} M (c, f) concentrations of the model antibodies BP53-12 and PAb 1801. In addition, the threshold levels for burst collection are given. The data were grouped into 1 ms time intervals. Excitation energy at the sample: 250 μ W. g) Binding isotherm, that is, number of fluorescence bursts above a threshold of 30 kHz (burst rate, ν_b) obtained from a 5×10^{-11} M solution of epitope I in the presence of different antibody concentrations (BP53-12).

small burst sizes with count rates (photon counts s^{-1}) of up to ~ 20 –30 kHz under the applied laser excitation energy of 250 μ W (Figure 3a,d). Binding to the antibody induces a conformational change in the peptide chain leading to reduced charge-transfer interactions. Therefore, higher fluorescence burst rates (bursts per time) and burst sizes with count rates of up to 100 kHz are observed (Figure 3b, c, e, f). The slightly smaller number of fluorescence bursts detected from epitope II (Figure 3e, f) indicates a lower binding affinity to the antibody. To count the number of bursts above a certain threshold we used an automated burst recognition procedure. To suppress bursts of quenched (unbound) epitopes efficiently, only bursts with a count rate of higher than 30 kHz and 20 kHz for epitope I and II, respectively, were used. The starting and end point of a burst were defined by a count rate of 5 kHz. This procedure results in a background burst rate of 0.04 Hz for the two labeled epitopes. Counting of all fluorescence bursts above these threshold levels provides an easy and rapid way to increase the assay sensitivity. Figure 3g shows the binding isotherm obtained from a 5×10^{-11} M solution of epitope I in the presence of different concentrations of the mouse antibody BP53-12. At a background burst rate of 0.04 Hz, an acquisition time of 3 min is sufficient to detect 10^{-11} M model antibody on the basis of a sixfold increased burst rate (0.24 bursts s^{-1}). Under saturation conditions, that is, 10^{-8} M model antibody, the burst rate increases 62.5-fold (2.50 Hz, Figure 3g). The error of the determined burst rates is mainly controlled by the acquisition time. The relative error in the measured burst rates, ν_b , is proportional to $N^{-1/2}$ for N bursts recorded over an infinite time window, that is, for a burst rate of 2.5 Hz calculated from 450 detected bursts in 3 min, the error is negligible. For smaller burst rates, for example, 0.24 Hz, the error is in the range of 15%. Unlike in the single-molecule measurements, the fluorescence intensity increased only approximately twofold in ensemble measurements. The substantially enhanced discrimination between quenched and unquenched peptide epitopes demonstrates the advantage of single-molecule spectroscopy for diagnostic applications.

To answer the question whether the developed peptide-based molecular probes can be utilized for early-stage detection and follow-up of malignant diseases directly in human sera, that is, whether the epitopes are recognized by human p53-autoantibodies, we undertook a study with serum samples from tumor patients and healthy donors. As potentially positive probes we tested sera of 40 breast tumor patients. All samples were allowed to equilibrate for one hour at room temperature with a 10^{-11} M solution of both epitopes.

Figure 4a and 4b show the time-dependent fluorescence intensities obtained from a 1:10 and 1:100, respectively, diluted serum sample from a healthy donor; Figures 4c, 4d, and 4e represent the fluorescence traces obtained from one of the positive tested serum samples. While the sera of healthy persons exhibit burst sizes of < 60 kHz for 1:10 dilutions, and < 30 kHz for 1:100 dilutions, the sera of 8 of the 40 breast tumor patients showed considerably higher fluorescence bursts, which can be easily identified among the signals of the free epitopes and the autofluorescence (Figure 4c–e). For serum measurements the threshold level for efficient discrim-

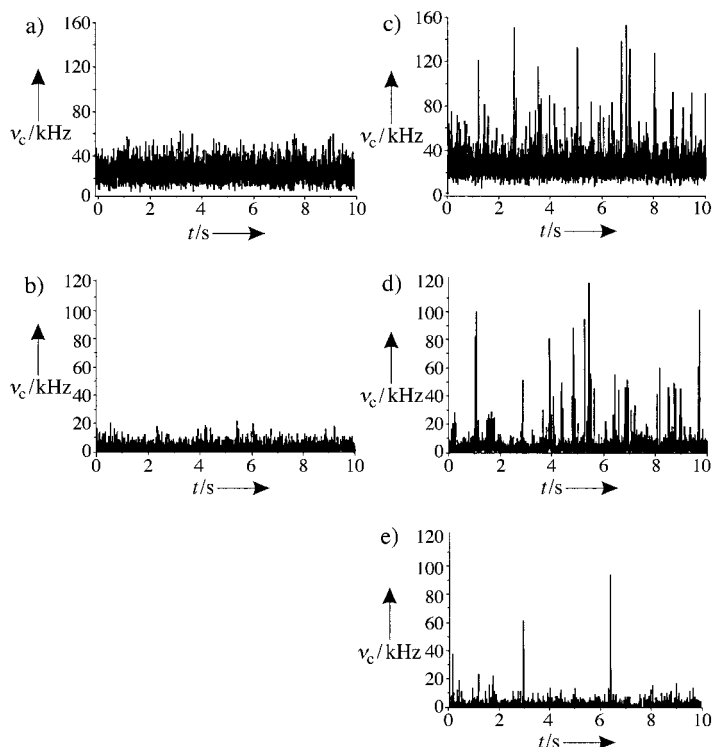


Figure 4. Time-resolved fluorescence intensities observed from a 1:1 mixture of both labeled epitopes (5×10^{-11} M) in diluted human serum samples. a) 1:10 and b) 1:100 dilutions of a serum sample from a healthy donor. c)–e) 1:10, 1:100, and 1:1000 dilutions, respectively, of a serum sample from a breast cancer patient with proven p53 accumulation in the tumor tissue.

ination between positive and negative signals must be adjusted with respect to the autofluorescence intensity, that is, the dilution of the sera. For example, for 1:100 or 1:1000 serum dilutions a threshold level of 30 kHz was used, while 1:10 dilutions require a threshold level of about 60 kHz. Figure 4e demonstrates that, even in the 1:1000 dilution of a positive serum, p53-autoantibodies are unequivocally identified by the measured burst rate of 0.16 Hz. For negative serum samples burst rates of 0.01–0.05 Hz were obtained by using the same burst recognition procedure.

To compare the results with heterogeneous assay formats, we performed ELISA tests with the same samples using recombinant p53 as antigen at similar serum dilutions. As can be seen in Figure 5, the achievable sensitivity and the dynamic range of our new molecular probes and the conventional ELISA test are comparable. Unspecific adsorption of serum proteins at the microtiter plate surface and subsequent binding of secondary detector antibodies complicates the use of the ELISA at serum dilutions lower than 1:100. By contrast, the new homogeneous assay permits measurements also in only slightly diluted serum samples (Figure 4c). As the homogeneous assay requires an incubation time of only one hour it is also considerably faster than the heterogeneous ELISA test which requires several additional time-consuming washing and incubation steps. Furthermore, the synthesis of large quantities of peptide-based molecular probes is uncomplicated and inexpensive compared to the use of recombinant p53. Since more than 90 % of p53-autoantibody positive sera

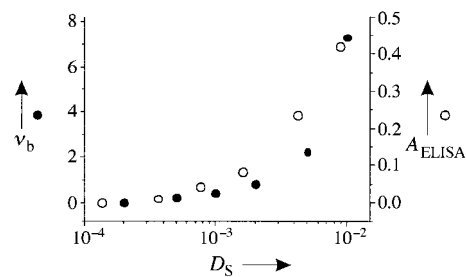


Figure 5. Direct comparison of the sensitivity and dynamic range of the new homogeneous assay (burst rate, v_b , that is, mean number of bursts per second above a threshold of 30 kHz averaged over 400 s) and the conventional heterogeneous ELISA (relative absorption measurement at 450 nm after enzymatic amplification, A_{ELISA}) measured from the same serum sample at different serum dilutions, D_s . Nonspecific adsorption and subsequent binding of the secondary detector antibodies prevent the use of the ELISA for serum samples diluted less than 100-fold.

of patients with various cancer types react with at least one of the two investigated immunodominant N-terminal epitopes,^[4] the presented homogeneous assay might be useful for high-throughput screening of p53-autoantibodies within several minutes. Moreover, by monitoring the time-dependent burst rate, the presented technique permits the direct determination of binding kinetics. Finally, the use of single-molecule spectroscopy offers an elegant method for efficient discrimination between species, which emit different fluorescence intensities. In the experiments described here, we did not focus on the clinical value of the developed assay. Rather the results demonstrate that the use of rationally designed labeled peptide-based molecular probes in homogeneous fluorescence assays and single-molecule detection in the red spectral region can open new avenues for early-stage detection and follow-up of malignant diseases directly in human serum samples.

A study of the specificity of the assay for real clinical p53-autoantibody tests is currently in progress. Unfortunately, a simple comparison of the results obtained with our new assay and conventional ELISA assays is not straightforward. It has been shown that different ELISAs do not always give consistent results for the same serum sample.^[11] This problem is probably due to the utilization of different antigens, different cut-off levels, and different surface immobilization and passivation techniques. Our new homogeneous assay raises hope that these problems can be circumvented.

Experimental Section

The N-terminal labeling of the peptides with the fluorescent dye was performed by classical *N*-hydroxysuccinimide ester (NHS-ester) chemistry using standard solvents purchased from Merck (Darmstadt, Germany). The oxazine dye MR121 ($1 \mu\text{mol mL}^{-1}$) and the synthetic peptides ($1 \mu\text{mol mL}^{-1}$) were dissolved in dimethylformamide (DMF). The dye solution ($10 \mu\text{L}$, 10 nmol) was added to the peptide ($100 \mu\text{L}$, 100 nmol; tenfold excess) and diisopropylethylamine (DIPEA; $2 \mu\text{L}$). The solution was incubated for 3 h at room temperature in the dark. The N-terminal conjugate was purified by reversed-phase HPLC (Hypersil-ODS column, Knauer, Berlin; HPLC: Agilent Technologies, Waldbronn, Germany) using a linear gradient of 0–75 % acetonitrile in 0.1 M aqueous triethylammonium acetate. Reaction yields of the N-terminal products of about 55 % were achieved. Purity of the probes was checked by capillary gel electrophoresis. For antibody binding studies and serum measurements, the premixed solutions (assay buffer: 0.1 M sodium phosphate pH 7.7, 0.3 mg mL^{-1} hen

eggwhite albumin, 0.05 % Tween 20) of antibody or serum and probe were allowed to equilibrate for 1 h at room temperature in the dark. The p53-autoantibody ELISA kit was purchased from Dianova (Hamburg, Germany). Assays of the serum dilutions were performed following exactly the experimental protocol purchased with the kit. Relative fluorescence quantum yields, Φ_{rel} , were measured with respect to the fluorescence intensity of the free dye. Ensemble fluorescence lifetimes τ were measured with a standard spectrometer from IBH (model 5000 mC; Glasgow, UK) for time-correlated single-photon counting (TCSPC) using a pulsed diode laser (635 nm) as excitation source (4096 channels \times 12.5 ps, 5000 photons in the maximum channel). To exclude polarization effects, fluorescence was observed under the magic angle (54.7°). The decay parameters were determined by least-square deconvolution, and their quality was judged by the reduced χ^2 values, and the randomness of the weighted residuals. In the case that a monoexponential model was not adequate to describe the measured decay, a multiexponential model was used to fit the decay [Eq. (1)]. Here a_i are the pre-exponential factors that describe the ratio of

$$I(t) = I(0) \sum a_i \tau_i \quad (1)$$

the excited species, and τ_i denote their lifetimes. Owing to the limited time resolution strongly quenched populations with decay times shorter than about 50 ps are not revealed.

The set-up for the single-molecule experiments consists essentially of a standard inverse fluorescence microscope equipped with a pulsed diode laser emitting laser pulses at 635 nm (100 ps FWHM) with a repetition rate of 64 MHz, (Picoquant, Berlin, Germany). The collimated laser beam was coupled into an oil-immersion objective (100 \times , NA 1.4; Nikon, Japan) by a dichroic beam splitter (645DLRP; Omega Optics; Brattleboro, VT, USA). The average laser power was adjusted to be 250 μ W at the sample. The fluorescence signal was collected by the same objective, filtered by a band-pass filter (675RDF50; Omega Optics; Brattleboro, VT, USA), and imaged

onto a 100- μ m pinhole oriented directly in front of an avalanche photodiode (AQR-14; EG&G, Canada). The detector signal was registered by a PC plug-in card (SPC-630; Becker&Hickl, Berlin, Germany). The pre-mixed samples were transferred onto a microscope slide with a small depression and covered by a cover slip.

Received: June 18, 2002

Revised: October 15, 2002 [Z19549]

- [1] T. Soussi, *Immunol. Today* **1996**, 17, 354–356.
- [2] D. P. Lane, *Nature* **1992**, 358, 15–16.
- [3] a) J. M. Nigro, S. J. Baker, A. C. Preisinger, J. M. Jessup, R. Hostetter, K. Cleary, S. H. Bigner, N. Davidson, S. Baylin, P. Devilee, *Nature* **1989**, 342, 705–708; b) M. Hollstein, D. Sidransky, B. Vogelstein, C. C. Harris, *Science* **1991**, 253, 49–53.
- [4] R. Lubin, B. Schlichtholz, D. Bengoufa, G. Zalcmann, J. Trédaniel, A. Hirsch, C. Caron de Fromentel, C. Preudhomme, P. Fenaux, G. Fournier, P. Mangnin, P. Laurent-Puig, G. Pelletier, M. Schlumberger, F. Desgrandchamps, A. Le Duc, J. P. Peyrat, N. Janin, B. Bressac, T. Soussi, *Cancer Res.* **1993**, 53, 5872–5876.
- [5] J. Bartek, J. Bartkova, J. Lukas, Z. Staskova, B. Vojtesek, D. P. Lane, *J. Pathol.* **1993**, 169, 27–34.
- [6] L. Banks, G. Matlashewski, L. Crawford, *Eur. J. Biochem.* **1986**, 159, 529–534.
- [7] S. Nie, D. T. Chiu, R. N. Zare, *Science* **1994**, 266, 1018–1021.
- [8] M. Sauer, C. Zander, R. Mueller, B. Ullrich, K. H. Drexhage, S. Kaul, J. Wolfrum, *Appl. Phys. B* **1997**, 65, 427–431.
- [9] S. Weiss, *Science* **1999**, 283, 1676–1683.
- [10] M. Sauer, B. Angerer, W. Ankenbauer, Z. Foldes-Papp, F. Goebel, K. T. Han, R. Rigler, A. Schulz, J. Wolfrum, C. Zander, *J. Biotechnol.* **2001**, 86, 181–201.
- [11] M. Montenarh, *Dtsch. Med. Wochenschr.* **2000**, 125, 141–143.